Manuscript Details

Manuscript number	IJHEH_2020_313_R1
Title	Probabilistic Model for Quantitative Risk Assessment of COVID-19: the case of a patchy environment with potential for migration between continents
Article type	Full Length Article

Abstract

Although many strategies have been discussed by world health authorities to control the spread of COVID-19, the microbial risk to the world population associated to such strategies remains unclear. Then, we conducted a Quantitative Microbial Risk Assessment (QMRA) to predict relative risks for future scenarios and evaluate the effectiveness of different management actions from March 17th 2020 to March 16th 2021. We have developed a probabilistic model to quantify the risks of the novel coronavirus explosion (i.e. more than 25% infections in the world population, a rate similar to that of the “Spanish Flu”). By means of this model, we carried out a QMRA for a variety of scenarios, including the social isolation of young and/or elderly people, travel restrictions and using medical tools, all of which help reduce deaths. We quantified, categorized and ranked the risks for each scenario. We estimated that, in the absence of interventions, COVID-19 would have: a 100% risk of explosion; this would most likely occur in nine weeks; would lead to an expected infection rate of 34% (2.6 billion) of the world population and 67 million deaths until mid-March 2021; and Africa would be the continent with the largest expected number of infected people. We validated the model by means of comparison of real against predicted values from March 17th to April 28th 2020 and showed that the results for this period are consistent with a business as usual scenario in Asia and moderate mitigation in all the other continents. If everything went on like this, we would have 55% risk of explosion, expected infection rate of 22% (1.7 billion) of the world population and 22 million deaths until mid-March 2021. Finally, strong mitigation actions in all continents could reduce these numbers to: 7% risk of explosion, infection rate of 3% (223 million) of the world population and 1.5 million deaths.

Keywords	novel coronavirus; COVID-19; quantitative microbial risk assessment; probabilistic modelling; stay at home.

Corresponding Author	Heitor Oliveira Duarte
Corresponding Author's Institution	Federal University of Pernambuco
Order of Authors	Heitor Oliveira Duarte, Paulo Gabriel Siqueira, alexandre oliveira, Marcio das Chagas Moura
Suggested reviewers	Marcelo Martins, Andrew Robinson, Enrique Droguett, Tatiane Micheletti, Paulo Mangini, Roger Flage, Piero Baraldi, Marilia Ramos

Submission Files Included in this PDF

File Name [File Type]

cover letter covid.docx [Cover Letter]

Response to reviewers for submission.docx [Response to Reviewers]

revised paper for submission (3).docx [Manuscript File]

Figures revised for submission.docx [Figure]

Tables revised for submission.docx [Table]

Supplementary Material (SM) QMRA of COVID-19 (1).docx [Supplementary Material]

To view all the submission files, including those not included in the PDF, click on the manuscript title on your EVISE Homepage, then click 'Download zip file'.

Probabilistic Model for Quantitative Risk Assessment of COVID-19: the case of a patchy environment with potential for migration between continents

Heitor O. Duarte[a*]; Paulo G. S. C. Siqueira[b,c*]; Alexandre C. A. Oliveira[a]; Márcio J. C. Moura[b,c]

*Corresponding authors

Email: heitorod@gmail.com; psems@hotmail.com; calumbi-oliveira@hotmail.com; marcio@ceerma.org

[a]Department of Mechanical Engineering, Universidade Federal de Pernambuco, Av. Prof. Moraes Rego, 1235 - Cidade Universitária, Recife - PE, 50740-550

[b]CEERMA - Center for Risk Analysis, Reliability Engineering and Environmental Modeling, Universidade Federal de Pernambuco, Recife-PE, Brazil

[c]Department of Industrial Engineering, Universidade Federal de Pernambuco, Rua Acadêmico Hélio Ramos, s/n, Cidade Universitária, CEP: 50740-530 Recife-PE, Brazil

Abstract

Although many strategies have been discussed by world health authorities to control the spread of COVID-19, the microbial risk to the world population associated to such strategies remains unclear. Then, we conducted a Quantitative Microbial Risk Assessment (QMRA) to predict relative risks for future scenarios and evaluate the effectiveness of different management actions from March 17th 2020 to March 16th 2021. We have developed a probabilistic model to quantify the risks of the novel coronavirus explosion (i.e. more than 25% infections in the world population, a rate similar to that of the "Spanish Flu"). By means of this model, we carried out a QMRA for a variety of scenarios, including the social isolation of young and/or elderly people, travel restrictions and using medical tools, all of which help reduce deaths. We quantified, categorized and ranked the risks for each scenario. We estimated that, in the absence of interventions, COVID-19 would have: a 100% risk of explosion; this would most likely occur in nine weeks; would lead to an expected infection rate of 34% (2.6 billion) of the world population and 67 million deaths until mid-March 2021; and Africa would be the continent with the largest expected number of infected people. We validated the model by means of comparison of real against predicted values from March 17th to April 28th 2020 and showed that the results for this period are consistent with a business as usual scenario in Asia and moderate mitigation in all the other continents. If everything went on like this, we would have 55% risk of explosion, expected infection rate of 22% (1.7 billion) of the world population and 22 million deaths until mid-March 2021. Finally, strong mitigation actions in all continents could reduce these numbers to: 7% risk of explosion, infection rate of 3% (223 million) of the world population and 1.5 million deaths.

Keywords

novel coronavirus; COVID-19; quantitative microbial risk assessment; probabilistic modelling; stay at home.

Introduction

The World Health Organization (WHO) has declared the coronavirus disease (COVID-19), which is caused by the severe acute respiratory syndrome coronavirus 2 (SARS-CoV-2), a pandemic (WHO, 2020a). Indeed, it has been confirmed that there are infected people in all the six continents, i.e.: Europe (EU), North America (NA) (Canada, United States and Mexico), South America (SA) (all other countries in America including Central America), Asia (AS), Africa (AF) and Oceania (OC). It is a worldwide threat in which all countries and continents must come together as one against a common enemy.

Quantitative Microbial Risk Assessment (QMRA) is the formal process of estimating the probability of undesired consequences to humans due to exposure to one or more microbial pathogens (Duarte et al, 2019; Haas et al., 1999). The main objective of a QMRA is to predict relative risks for future scenarios and/or to evaluate the effectiveness of different containment measures (Duarte et al., 2019).

Many strategies have been discussed and implemented in a bid to control the spread of the virus until a vaccine is developed, licensed and manufactured at a global scale. These actions include restrictions on travel and business/studies/social activities (hereinafter, the term business will be used to refer to all three types of activity), social isolation (for the purposes of this work, this is equivalent to 'stay at home' measures), vertical isolation (i.e., when it affects only the elderly and groups at risk), and using therapeutics and new medical tools to reduce fatality rates (hereinafter, the term 'medical tools' will be adopted and this includes the use of therapeutics).

Most decisions are taken based on the subjective opinions of epidemiologists (Kupferschmidt and Cohen, 2020; Sohrabi et al., 2020; Toms and Petrie, 2020) or projections of deterministic models (Altaf and Atangana, 2020; T. M. Chen et al., 2020; Choi and Ki, 2020; Ferguson et al., 2020; Peng et al., 2020; Walker et al., 2020), but neither the risks associated to these decisions, nor the uncertainties in the opinions and estimates have been quantified. In this sense, a recent study highlights the importance of acknowledging uncertainty as a main component of risk, in order to properly characterize and communicate risk (Aven and Bouder, 2020). Globally, policymakers are demanding tools to guide them on how to prioritize resources for designing control strategies. Indeed, they require objective answers for questions such as:

- How many people may die in the world and how many may be infected if we decide on strategy A, B or C for the next one year?
- By what amount and for how long is the social isolation of young and/or elderly people necessary to reduce risk to a low or negligible level?
- To what extent and for how long are restrictions on intercontinental flights necessary to reduce risk to a low or negligible level?
- Which continents are at risk in the future? Which one deserves the most effort to control the disease? What is the order of prioritization?

Generally, to model the dynamics of a disease, such as those involved in the transmission of SARS-CoV-2, some simplifying assumptions are necessary. For example, traditional approaches for modeling COVID-19 are based on deterministic models that often rely on average data, and thus only provide expected results. These neither propagate the variability and uncertainty of data nor do they consider environmental stochasticity (i.e., the unpredictable natural fluctuation in vital rates (Fujiwara and Takada, 2017). As deterministic models for SARS-CoV-2 (Altaf and Atangana, 2020; T. M. Chen et al., 2020; Choi and Ki, 2020; Ferguson et al., 2020; Peng et al., 2020; Walker et al., 2020) lack stochasticity in parameters and uncertainty in results, potentially misleading conclusions may lead to imprudent decisions, which in turn, might lead to a much greater number of lives being threatened and lost.

One probabilistic model for SARS-CoV-2 was used for assessing the risk of outbreaks outside China (Boldog et al., 2020) when the disease was still not considered a pandemic. This model made predictions from 23rd January until 15th March 2020 and presented suggestions for control measures (e.g., travel restrictions from China) to countries at risk. However, serious limitations of

this study include: (i) it was conducted at the beginning of February 2020 when most infected people were still in China, and thus it could simulate the spread of the disease only from China; (ii) it does not separate age groups; (iii) it does not quantify the number of deaths, but only cases of infection; (iv) it does not consider social isolation as a control measure.

Another characteristic of our model is that it represents COVID-19 globally. All the aforementioned models described COVID-19 dynamics in a single country or city. At the best of authors' knowledge, (Walker et al., 2020) provided the only model that predicts the global impact of COVID-19 and evaluates strategies for mitigation and suppression. Indeed, (Walker et al., 2020) deterministically predicted the number of infections and deaths in the world in seven different regions for the next 250 days for varying scenarios. However, (Walker et al., 2020) cannot be adopted for QMRA purposes, because they used only single point estimates for the number of infections and deaths. Thus, such an approach often leads to unrealistic estimates due to the inherent uncertainty that typifies these predictions (EPA, 1998).

On the other hand, probabilistic models are able to consider uncertainty in parameters and to give risk results in terms of probabilities. Using Monte Carlo simulations, for example, allows us to obtain a set of results for infections/deaths so that a non-parametric probability distribution can be drawn, which accommodates uncertainty i.e., there is a probability associated to each estimate of infections/deaths at a time *t*. With such an approach, a model can successfully quantify risks as a measure of the probability of undesired consequences (infections/deaths), thus, supporting decision makers in understanding the likelihood of the outcomes of an action, and making informed decisions. Therefore, the aim of this paper is to develop an epidemiological model for COVID-19 at the world-population-level that overcomes the aforementioned drawbacks and is tailored for a QMRA. We set out to answer the aforementioned questions. To the best of our knowledge, this paper conducts the first QMRA of COVID-19 at population-level worldwide.

The remainder of this paper is organized as follows. First, we present the structure of the model and assumptions, which is flexible in parameterization and so can be used to simulate varying scenarios. Next, we discuss the materials and methods used to conduct a QMRA by means of this model. We then present results for representative scenarios, validate the model and discuss its advantages and limitations. Finally, some conclusions are drawn and suggestions are made for future research.

The structure of the model and assumptions

Our proposed model is probabilistic in nature, and thus provide meaningful information to decision makers because it allows for: (i) the assessment of uncertainty by specifying lower and upper bounds in the results; (ii) modeling the spatial dynamics of infected people across six continents; (iii) the quantification of the risk of explosion (i.e., the number of infected people increases to over 25% of the world population after 12 months). The 25% threshold for the risk of explosion was defined based on the most severe pandemic in the 20th century, namely the Spanish Flu, which lasted from January 1918 to December 1920, (caused by the A(H1N1) virus). It is estimated to have infected 500 million people, approximately 25% of the world population at that time, and to have caused 20-50 million deaths (Spreeuwenberg et al., 2018; WHO, 2019, 2005).

These tasks may be performed for scenarios regarding different containment measures, thus assessing their effectiveness in terms of risk. By using this approach, it is also possible to identify the continents, where SARS-CoV-2 might persist, and hence this helps target public control strategies to reduce human infections in those areas.

To estimate the parameters of the model, data from the literature and public databases have been gathered to meet the requirements of the approach. Due to the lack of access to private data, some parameters (e.g., number of flights arriving every day in each country) were estimated for which simplifications had to be made.

Fig. 1 shows a simplified schematic representation of our model. We separate the world human population into three states: Susceptible; Infected; and Recovered. Then, we subdivide each state into two age groups: the Young ($<$ 60 years) and the Elderly ($\geq$ 60 years). When a Susceptible individual gets Infected, whether he or she is young or elderly, he/she stays in this state for a period of time, and then either becomes Recovered or dies (represented by the "Deaths Counter" box).

After recovery, a person can get Infected again with a very low probability (it is still unknown if a Recovered person gains 100% immunity (Lan et al., 2020)). The transition between states is governed by random variables that follow Probability Density Functions (PDFs) that vary over time, i.e., the parameters of the PDFs vary with time according to each scenario.

The world (metapopulation) is divided into six continents (subpopulations) with potential for dispersal among them. The dispersal rates from one continent to another also follow PDFs. We group countries into continents to keep the model and communication of risk simpler. A global model that represents dispersal among all countries could become intractable, resulting in challenging risk communication to authorities as well as to the public.

The structure of the proposed model can be tailored to incorporate many realistic and case-specific features, such as: (i) the spatial structure of the infected population at the global level over time with potential for dispersal among continents; (ii) the population structured by age range (young and elderly) with different probabilities of fatality and/or infection; (iii) control measures such as business restrictions and social isolation (reducing exposure), medical tools targeted at decreasing death rates and travel restrictions between continents. Table 1 and Table 2 present, respectively, descriptions of the variables and parameters.

The model describes a metapopulation consisting of six subpopulations in the continents of EU, NA, LA, AS, AF and OC, with potential for dispersal from one patch to another. The structure of the state of each population is [s=1] young susceptible, [s=2] young infected, [s=3] young recovered, [s=4] elderly susceptible, [s=5] elderly infected, and [s=6] elderly recovered, where *s* is the state. Dispersal is state-specific, which means we can simulate distinct dispersal rates for the young and elderly.

Let $I^i(t)$ denote the number of infected people in continent (patch) *i* at time *t,* and $N^i(t)$, the total population in *i* at time *t*. Then, the model forward projects the number of infected people, $I^i(t) = N_2^i(t) + N_5^i(t)$, (i.e. number of young infected $N_2^i(t)$; the number of elderly infected $N_5^i(t)$) for all *i*, for 52 weeks (1 year) from March 17th, 2020 to March 16th, 2021.

In population ecology, the density-dependence (DD) is the modification in the influence of any factor that affects population growth as the population density changes (Akçakaya et al., 1999; Burgman et al., 1993). In this paper, we did not aim at evaluating the growth in world population, and therefore population size is held constant (there are no inclusions of new susceptible young) and the DD type is considered as the ceiling. The basis for accounting for DD was the total subpopulation of each continent (susceptible+infected+recovered). However, DD was modeled to affect only the number of infected. Under this type of DD, the infected population exponentially grows until the total subpopulation (susceptible+infected+recovered) reaches the ceiling (e.g., when the number of susceptible individuals is so low and of recovered is so high that the number of infections stop growing). Then, it remains at that level until there is a decline in the total population (e.g., a random fluctuation or emigration) that takes it below the ceiling (Akçakaya et al., 1999; Akçakaya and Root, 2013).

Note that we consider no inclusions of new susceptible individuals (babies being born), but there are inclusions of the newly infected and, then, of newly recovered individuals, so DD matters because it limits the number of infected individuals; otherwise, this number would grow exponentially and infinitely. The ceiling is continent-specific, denoted by K^i, and is defined to be the total current subpopulation in that continent.

Given that, the following algorithm represents one replication for stochastically simulating the metapopulation model. For each iteration, repeat the following steps for all *i*:

a) Project population-specific state numbers:

$$\begin{bmatrix} N_1^i(t+1) \\ N_2^i(t+1) \\ N_3^i(t+1) \\ N_4^i(t+1) \\ N_5^i(t+1) \\ N_6^i(t+1) \end{bmatrix} = \begin{bmatrix} a_{11} & 0 & 0 & 0 & 0 & 0 \\ 0 & a_{22}^i(t) & 0 & 0 & a_{25}^i(t) & 0 \\ 0 & a_{32} & a_{33} & 0 & 0 & 0 \\ 0 & 0 & 0 & a_{44} & 0 & 0 \\ 0 & a_{52}^i(t) & 0 & 0 & a_{55}^i(t) & 0 \\ 0 & 0 & 0 & 0 & a_{65} & a_{66} \end{bmatrix} \times \begin{bmatrix} N_1^i(t) \\ N_2^i(t) \\ N_3^i(t) \\ N_4^i(t) \\ N_5^i(t) \\ N_6^i(t) \end{bmatrix} - \begin{bmatrix} 0 \\ \alpha_2 * N_2^i(t) \\ 0 \\ 0 \\ \alpha_5 * N_5^i(t) \\ 0 \end{bmatrix}$$

where a_{su} is the transition rate from state u to state s and a_{uu} is the permanence rate in state u (??, ?? $\in \{1,2,3,4,5,6\}$). For example, a_{32} is the transition rate from state 2 to 3 and a_{11} is the permanence rate in state 1. α_2 and α_5 are the periodic mortality of infected young and elderly individuals respectively.

b) Update projections to account for DD: $N^i(t+1) = max\{N^i(t+1); K^i\}$.

c) Update projections of $N^i(t+1)$ to account for the dispersal of individuals by adding the number of entries and subtracting the number of exits for each population:

$$\begin{bmatrix} N^{EU}(t+1) \\ N^{NA}(t+1) \\ N^{LA}(t+1) \\ N^{AS}(t+1) \\ N^{AF}(t+1) \\ N^{OC}(t+1) \end{bmatrix} = \begin{bmatrix} N'^{EU}(t+1) \\ N'^{NA}(t+1) \\ N'^{LA}(t+1) \\ N'^{AS}(t+1) \\ N'^{AF}(t+1) \\ N'^{OC}(t+1) \end{bmatrix} + [M]_{6x6} \begin{bmatrix} N'^{EU}(t+1) \\ N'^{NA}(t+1) \\ N'^{LA}(t+1) \\ N'^{AS}(t+1) \\ N'^{AF}(t+1) \\ N'^{OC}(t+1) \end{bmatrix} - [M]_{6x6}^{T} \begin{bmatrix} N'^{EU}(t+1) \\ N'^{NA}(t+1) \\ N'^{LA}(t+1) \\ N'^{AS}(t+1) \\ N'^{AF}(t+1) \\ N'^{OC}(t+1) \end{bmatrix}$$

where $[M]_{6x6}$ is a matrix comprising the dispersal rates (m_{ij}) of individuals from continent j to continent i. Note that some transition rates (i.e., a_{11}, a_{22}, a_{32},a_{33},a_{44},a_{65},a_{65}) are random variables that follow PDFs with parameters that are constant over time; therefore, a value is randomly selected from the associated PDF for an iteration and kept constant for the entire 52 time-steps of this iteration. Other transition rates (i.e., $a_{22}^i(t), a_{25}^i(t), a_{52}^i(t)$ and $a_{55}^i(t)$) are nonparametrical stochastic processes because they are both random and dependent on the interaction among individuals; therefore, their PDFs change over time and a value is randomly selected from the associated PDF at time *t*.

RAMAS Metapop v.6.0 software (Akçakaya and Root, 2013) was adopted for running the simulations with 10,000 replications. This software is not itself a model, but a computational tool for constructing a metapopulation model and probabilistic simulation via the Monte Carlo method (Kalos and Whitlock, 2008). We share all the model files in RAMAS format (Duarte et al., 2020) .

Materials and data

QMRA methodology

We used the structure of the model presented to conduct a QMRA for COVID-19 by using the following steps (Duarte et al., 2019): (i) characterize the problem; (ii) describe the scenarios (SCNs); (iii) assess exposure; (iv) assess frequency; (v) parameterize the model and initial conditions; and (vi) quantify and categorize the risks. (Duarte et al., 2014) already applied this methodology to run QMRA for schistosomiasis disease.

Quantitative Risk Assessment (QRA) is closely linked to risk communication (i.e., the effective transfer of technical information regarding possible risks to nontechnical audiences) (Teaf and Kuperberg, 2004). The way risk is conceptualized and described could be very important for how the authorities judge the magnitude of the risk, communicate the risk to the public and conclude what to do (Aven and Bouder, 2020). It is almost useless to quantify risks if they cannot be well understood by the non-technical audience, as is the case of many world policymakers (since they are not experts on the language of probability). As to risk categories, quantified risk can be transformed into risk classes that are easier to interpret.

Therefore, risk categories have been used in all fields of QRA to make risk communication easier (e.g., industrial QRA (CPR18E, 2005), ecological QRA (IUCN, 2001), microbial QRA for water

safety management (WHO, 2016), microbial QRA of schistosomiasis (Duarte et al., 2014). Yet, surprisingly, there is still no consensus in the literature on how to categorize the quantified risk of the explosion of a pandemic at population-level. Thus, we here propose four risk categories and the correct understanding of these is vital for a correct interpretation of the results:

- CRITICAL RISK (CR): >50% probability of explosion within 6 weeks.
- HIGH RISK (HI): >20% probability of explosion within 12 weeks.
- CONSIDERABLE RISK (CO): >10% probability of explosion within 52 weeks.
- NEGLIGIBLE RISK (NE): <10% probability of explosion within 52 weeks.

The method for reaching the above categories is as follows. Quantitative risk has three dimensions: probability, undesired consequence, and time (Duarte et al., 2019; IUCN, 2001), and then we established bounds for these three dimensions in order to form a risk category. In our case, the undesired consequence is the explosion of the disease (more than 25% infected people in the world at time *t*, similarly to the Spanish Flu); this threshold is the same for all categories. Regarding the probability dimension, the bounds are the same as in the red list categories of the International Union for the Conservation of Nature (IUCN) (IUCN, 2001) (i.e., >50%, >20%, >10% and <10%, respectively for CR, HI, CO and NE). With respect to the time dimension, it is also based on the IUCN categories (i.e., 10, 20, 100 and 100 years, respectively for CR, HI, CO and NE), but adapted to the time horizon in which we make the forecast (i.e., 52 weeks). Thus, we have 6, 12, 52 and 52 weeks for CR, HI, CO and NE respectively.
Note that the proposed categories do not consider the probability of massive deaths as is common in industrial QRA. Our categories seek indicating the risk of overloading the health system, which is associated not only with deaths, but also with high numbers of sick people and substantial societal and economic costs. Conversely, risk categories based on deaths could neglect very infectious disease with low rates of death, although the health system would be overloaded. Thus, we preferred to consolidate our undesired consequence in terms of infections, as these categories can serve as a basis for QMRA of future pandemics and these will not neglect infectious diseases with low rates of death but high rates of infection.

Characterizing the problem

The problem consists of quantitatively assessing the risks of SARS-CoV-2 in order to provide health managers worldwide with objective answers about the dynamics of the disease under several control strategies. To ensure that the results of this study would meet managers' needs, we chose as assessment endpoints: the number of infected people; and the number of deaths. This evaluation is based on a probabilistic model that provides risk results as a PDF for those endpoints over time, with an average value and a confidence interval.
This QMRA is intended to be conservative in the sense that it does not underestimate risks. Then, whenever different sources provided different parameters estimates for the PDF that governs a transition rate, a_{su}, we considered the most conservative ones. The outputs of this QMRA are as follows: (i) projection of the infected subpopulation over time for each continent and in the world (metapopulation) for 52 weeks; (ii) projection of the accumulated number of deaths in the world over time for 52 weeks; (iii) risk curves of explosion; (iv) time to explosion; (v) risk categorization; and a (vi) comparison of these results for all scenarios defined in the next section.
Data regarding the number of infected people for each day, from Jan 1st 2020 until Mar 23rd 2020, for each country, was gathered from the public database managed by the Johns Hopkins University Center for Systems Science and Engineering (JHU CSSE) (JH, 2020). The raw data is also available in the SM Appendix, Table A1. The main sources of information used for a general qualitative understanding of the SARS-CoV-2 dynamics were (Altaf and Atangana, 2020; P. Chen et al., 2020; Choi and Ki, 2020; Ferguson et al., 2020; Lin et al., 2020; Pang et al., 2020; Walker et al., 2020; World Health Organization (WHO), 2020b). The specific source of information used for estimating each specific parameter of the model is presented in Table 2.

Description of scenarios

It is quite intricate to predict/assess all the potential events (e.g., meteorological and environmental conditions, numerous control strategies, various novel medical tools, changes in hygiene and cleaning culture, transportation restrictions in all modes, and events like virus mutation) that might occur in the future and influence SARS-CoV-2 transmission. Thus, our model does not aim to be precisely predictive, only descriptive.
In this context, we defined three scenarios (SCNs) and compare them against a benchmark (SCN-0) so that we can evaluate changes in SARS-CoV-2 dynamics (and the reduced/added risk) caused by each scenario. The benchmark scenario (SCN-0) is defined as follows:

- Do-nothing plan;
- Business as usual;
- No social isolation neither for the young nor the elderly (100% exposure);
- No travel restrictions;
- No new medical tools to reduce death rates.

To assess the efficiency of integrated containment strategies without excessive information to represent the many possible combinations, we evaluated three scenarios, which we believe to be representative for the next year:

- Moderate mitigation (SCN-1):
  - Social isolation of the young (assumed 18% exposure) and the elderly (assumed 9% exposure) for the next 2 and 6 weeks respectively. Thereafter, exposures go back to 100%;
  - 75% reduction in intercontinental flights in the next 6 weeks, and thereafter flights are back with a 25% reduction in the usual volume;
  - Medical tools targeted at reducing fatality rates by 50%;
  - *Ceteris paribus* SCN-0.
- Strong mitigation (SCN-2):
  - Social isolation of the young (assumed 18% exposure) and the elderly (assumed 9% exposure) for the next 7 and 17 weeks respectively. Thereafter, exposures go back to 100%;
  - 75% reduction in intercontinental flights in the next 12 weeks, and thereafter flights are back with a 25% reduction in the usual volume;
  - Medical tools targeted at reducing fatality rates by 75%;
  - *Ceteris paribus* SCN-0.

The rationale for the exposure levels in each scenario will be further explained in the next section. Also, there has been much discussion about the so-called vertical isolation, which affects only the elderly and groups at risk. The strategy is criticized by international health organizations, but is defended by some politicians (Time24, 2020). To evaluate the effectiveness of this strategy, we analyzed one more scenario.

- Vertical isolation (SCN-3):
  - Business as usual for all the young (100% exposure);
  - The elderly completely isolated (0% exposure) during 1 year;
  - 100% travel restriction for the elderly;
  - *Ceteris paribus* SCN-0.

Exposure Assessment
Human exposure to SARS-CoV-2 mostly occurs when people leave home in their day-to-day life. In a business as usual scenario (SCN-0), we assume the young are out for business 46 hours/week and the elderly for 23 hours/week. Thus, we set this level of exposure for our benchmark as 100% for the young and 50% exposure for the elderly. Then, we make changes in the exposure level in order to represent social isolation in mitigation scenarios. Table 3 shows a summary of the exposure assessment.

Frequency assessment

When exposed to infected individuals, a susceptible individual may get infected. We name this process the frequency of infection. The frequency of infection per week, μ^i, can be estimated by processing the data on the daily number of confirmed cases in each country provided by (JH, 2020) (SM Appendix, Table A1). To that end, we grouped countries into continents. Then, we calculated the weekly frequency of infection in each continent for every day D (i.e., the number of infected people in $t+7$ divided by the number of infected people in t). From this sample of values, we calculated the mean and standard deviation in each continent and checked if there were outliers outside a 99.7% CI ($\mu \mp 3\sigma$). If there were outliers, we calculated μ and σ and checked for outliers again. We repeated this process for each continent until there were no more outliers. Table 4 presents the frequency of infection per patch, which represents a do-nothing scenario (SCN-0).

After an individual gets infected, (s)he may either die or recover. For the fatality rate (α_Y,α_I) (i.e., the frequency of the rate at which infected individuals may die per week), we use as reference a study that presented the fatality rates in the world per age group deciles, i.e.: 0-9, 10-19, …, 70-79, until >80 years old (Vital Surveillances, 2020). We grouped fatality rates into our age classes of interest (<60 and ≥ 60 years old), and then estimated age-specific fatality rates of the infected young and elderly, i.e., respectively: 0.006216 and 0.067575 per week. This means that on average 0.62% and 6.76% of the total number of infected young and elder population die per week respectively.

The recovery rates (a_{32},a_{65}) (i.e., the transition rate per week from infected to recovered) can be estimated based on the incubation and transmission period of those who develop symptoms. A study suggested that transmission of SARS-CoV-2 also occurs during the incubation period. Thus, recovery time can be considered as the sum of incubation and transmission periods. According to (Lauer et al., 2020), under conservative assumptions, most individuals take 14 days to recover. Thus, after 2 weeks, it is highly unlikely that an infected individual would still be in the transmission period. This is also in accordance with, and well supported by, the recommendation of the U.S. Centers for Disease Control and Prevention for the period of active monitoring of infected people (14 days = 2 weeks) (WhiteHouse, 2020). Thus, we estimated the mean recovery rate as $a_{32} = \left(\frac{1}{2}\,weeks\right) * (1-\alpha_2)$, for the young individuals (note that the same can be done for the elderly, by using a_{55} and α_5).

Parameterizing the model and Initial Conditions

Table 1 and Table 2 summarize the variables, parameters and initial conditions of the model. Some studies in the literature have already estimated parameters governing the dynamics of SARS-CoV-2, which we use in the proposed model: the fatality rate per age class (Vital Surveillances, 2020); the mean incubation and transmission period (Lauer et al., 2020); the time taken to recover (Lauer et al., 2020); and the proportion of the young and elderly infected (Population Pyramid, 2019). Other parameters were estimated from data (SM Appendix, Table A1): the frequency of infection per week for each continent. On the other hand, due to the unprecedented characteristic of this disease, there is still a lack of scientific information, and then two parameters of the model were estimated via conservative educated opinions of the authors, i.e.: the permanence rate in state 2 (young susceptible); and the permanence rate in state 4 (elderly susceptible) (see Table 2 for the rationale and assumptions regarding these parameters). The estimates for these two parameters may be improved when more information becomes available.

Some parameters were estimated using a mean value and others a mean and standard deviation (mean and σ columns in Table 2). To make the latter uncertain, we consider that they have a Normal distribution. One can make good use of a Gaussian approach in the vital rates of biological models because there is a reasonable reason for random values not to be too far away from average, i.e., there are biological limitations preventing very large deviations and natural forces from equilibrium that bring vital rates back to their average values (Taleb, 2007). For probabilistic simulation, RAMAS converts the parameters of a Normal distribution into the corresponding

Lognormal counterpart, which avoids bias resulting from truncation because all parameters are greater than zero.

We model dispersal in a straightforward way. Indeed, we did not have access to private data of all flight arrivals and departures per country. Public information available only shows the total number of arrivals per country and continent in 2017 and 2018 (UNWTO, 2019). From this dataset, we took the average number of arrivals per year and estimated the average number of arrivals per week by dividing it by 52 (the number of weeks in a year), for each continent. Thus, we model dispersal rates per week from continent j to continent i as $m_{ij} = \left(\frac{M_{ij}}{N^j}\right)T_r$, where M_{ij} is the number of arrivals in the continent i from the continent j per week, N^j is the total subpopulation of the continent j and T_r is the travel restriction management measure that can vary from 0 to 1. As a result, we had dispersal rates in the order of 10^{-3}, 10^{-4} and 10^{-5}. We built a dispersal matrix $[M]_{6x6}$ for SCN-0 (SM Appendix, Table A2), where $T_r(t) = 1$. T_r is dependent on each scenario (see Description of scenarios section) and varies over time as can be seen in SM Appendix, Fig. A1.

Although the current proportion of infected individuals is very low (less than 0.1%), we estimate the initial number of susceptible individuals by subtracting the number of infected individuals for each continent in each age class from the total population. The proportion of age classes was estimated based on available data regarding the age pyramid in each continent (Population Pyramid, 2019).The initial number of fatalities and recovered people were assumed as zero, because the proportion of fatalities is still low, and data about individuals recovered are scarce and difficult to collect.

Results

Here, we present the main risk results of each scenario and make a comparison between them. SCN-0 works as a baseline for comparing and quantifying the risk reduction caused by mitigation strategies.

The results for the population were given in the following structure: average, ± SD, maximum and minimum. Then, we also present these results as boxplots (Fig. 2) to show the global infected population at the final time-step of the SCN-0 simulation, which is useful to identify the most likely continents, where SARS-CoV-2 might increase. Based on the results, in the absence of interventions, AF is likely to be the continent with the largest number of infected people in the near future, followed by EU, SA, NA, OC and AS.

Fig. 3 illustrates the efficiency of integrated strategies (social isolation + flight restrictions + medical tools) for disease control: (A) a projection of the world infected population; (B) a projection of the accumulated number of deaths in the world; and (C) time to explosion (i.e., the cumulative probability distribution for the time taken for the percentage of infected people in the world to exceed 25%) for each scenario.

In Fig. 3A and 3B, results for each scenario are presented as mean values. For example, for SCN-2: the expected infected population in the world is estimated to be around 223 million; and the expected cumulative total number of deaths is expected to be around 1.5 million in 52 weeks.

Based on the results in Fig. 3C, it is possible to categorize the risks associated to each scenario (see Table 5): High (HI) for SCN-0, High (HI) for SCN-3, Considerable (CO) for SCN-1 and Negligible (NE) for SCN-2. Fig. 3C also shows that, compared to SCN-0, strong mitigation (SCN-2) greatly increases the time to explosion, whereas for moderate mitigation (SCN-1) and vertical isolation (SCN-3), although the time to explosion is increased, it is still within one year.

Other important results are as follows: SCN-1 (moderate mitigation) and SCN-2 (strong mitigation) cause the risk of explosion to be reduced by, respectively, 52.7% and 92.72% compared to SCN-0; the vertical isolation plan alone (SCN-3) does not significantly reduce this risk, when compared to SCN-0, and so it is not useful to maintain the prevalence rate below 25%.

In order to suggest a scenario of NE risk, which would have the least impact on the economy, a sensitivity analysis of gradual decreases in the length of isolation of the young in SCN-2 was carried out. This showed that the explosion risk is already considerable for 6 weeks or less, suggesting that 7 weeks is the minimum that the young should be isolated.

To account for continent-focused strategies, we simulated: business as usual in the most populated continent (AS) and moderate mitigation in the rest; strong mitigation in the continent predicted to be the most hard-hit (AF) and moderate mitigation in the rest; and strong mitigation in the two continents predicted to be the most hard-hit (AF and EU) and moderate mitigation in the rest Results showed that there were significant reductions in the explosion risks, although all of them were still within the CO risk region (see Table 5).

Validation of the model

Our results are consistent with the outcomes of the business-as-usual scenario of another COVID-19 global model (Boldog et al., 2020), i.e.: infections in the order of billions and deaths in the order of millions in the world. Moreover, six weeks elapsed between the date we generated results from the model and the first review of this paper. This has given us an opportunity to validate the model, i.e., to compare the predictions for each scenario with real values for this six-week period.

First of all, we compared the real values of infections in the first six weeks with the results for each scenario applied to all continents in a general manner. We observed that SCN-1 (moderate mitigation) in all continents is the one closest to what is really happening in the world in general (no different continent-specific scenarios). Fig. 4 shows, for each continent, the comparison of the number of infections at week 6 (Apr 28th 2020), where the black dots are real values and the boxplots on the left of each graph are the predicted results for SCN-1 in all continents. Note that there is a good approximation for all continents.

Not by accident, our model has the feature of being able to simulate different SCNs on different continents so that it can be used in practice as a tool to predict the consequences of continent-specific decisions. To validate this feature, we simulated a business as usual SCN-0 for AS and a moderate mitigation SCN-1 for all other continents. This is in accordance with many news from Mar 17th to Apr 28th (Bird et al., 2020; Machado, 2020; The Inquirer, 2020) that say that Asian countries have been reopening their business. The results are shown in the boxplots on the right of each continent-specific graph in Fig. 4. Note that now there is an even better approximation for all continents. This illustrates how the model can be calibrated as new information arises, and then can be adapted to anything new that happens in reality. Indeed, it allows fast simulation and fast generation of updated and more accurate results.
Finally, we validated our model at global-level using predictions for SCN-0 in AS and SCN-1 in all other continents. Fig. 5A and Fig. 5B show, respectively, the comparison of the predicted against real number of infections and deaths. Note that the predicted number of infections (Fig. 5A) present a very good approximation, which suggests that the results of the model are consistent with a business as usual scenario in AS and moderate mitigation in all the other continents. On the other hand, for the number of deaths (Fig. 5B), the real values are higher than the third quartile of the predicted boxplot for all the six time-steps, thereby indicating that our assumption of medical tools that would reduce death rates by 50% may not correspond to reality, at least for these last six weeks.

Discussion

In this section, we first discuss the advantages and then the limitations of using this model.

Advantages.
Our model proved to have great potential to be truly informative for decision-making, and not just one more deterministic prediction for managers to follow without understanding all the uncertainty around the data. Although the data are still very imprecise, our model was able to propagate uncertainty in the results and give answers in terms of a distribution of consequences associated to probabilities. For every Monte Carlo run, a "single-point estimate" for the discretized time to explosion (e.g. in weeks), *T*, was calculated. After many Monte Carlo runs (e.g. 10,000), we had a set of "single-point estimates" for the time to explosion and the number of occurrences of a "single-point estimate". Thus, we could calculate and present the probability of occurrence of each "single-point estimate" (e.g. *P(T) = number of occurrences of T/10,000*). Then, for each time *t*, it was possible to cumulate the probabilities of all *T* lower than *t*, which results in the Cumulative Distribution Function (CDF) for the time to explosion, i.e.: $F_T(t) = P(T \leq t)$. In summary, $F_T(t)$ means the probability that explosion will occur at or before a time *t*. This function was plotted in a graph (Fig. 3C). The great advantage of such an approach over deterministic analysis is that results show not only what could happen, but how likely each outcome is. For example, another study used Monte Carlo simulations to provide a risk graph that show the cumulative probability over time (days) of exporting at least a single infected case from mainland China via international travel. Although the objective and scope of that study was different from ours, it also shows how probabilistic models and Monte Carlo simulation can provide results that incorporate the indelible uncertainty in the dynamics of COVID-19 (Wells et al., 2020).
We used the past six weeks (March 17th to April 28st 2020) to validate the model by comparing real with predicted infections and our results, for SCN-0 in AS and SCN-1 in all the other continents, do indeed correspond to reality (Fig. 5). The continent-specific predicted vs. real number of infections (Fig. 4) also corresponds to reality for all continents. Note that we present results for several scenarios, so that one of them will probably correspond to reality. In fact, our model cannot make precise predictions of what will exactly happen in the future. Any model that tries to do that, most likely will miss some information because decisions are taken every day and change the future. Our model allows for fast simulation, so it can be used as a tool to predict the impact of decisions before they are taken, so that authorities of the most representative countries in each continent may be warned of the risks of their decisions to world health.

Finally, we proposed criteria to categorize the quantified risks of a pandemic at population-level, which can be useful not only for COVID-19 but also as a reference for categorizing risks of any pandemic in the future. At the best of authors' knowledge, there have been no suggestions in the literature so far on how to categorize such risks. The rationale behind the categorization was explained in the QMRA methodology section. Readers must ensure that they fully understand it in order to be confident that they can correctly interpret the results of the risk category.

Limitations.

In the present application of our model, we consider that the probability of a recovered individual being infected again is 0. Yet, there is evidence that recovered individuals may become infected again (Lan et al., 2020), although it is still not certain whether such individuals have really become reinfected or they were not infected before, but the test result was false positive. However, our model is flexible in parameterization, and this probability can be easily changed to a value greater than zero when more information becomes available.

There is the potential for bias in the fatality rates of the young and elderly if not everyone who has been infected are being diagnosed. A recent study showed that it is likely that this is happening and fatality rates are being underestimated (Baud et al., 2020). Consequently, the projection of the accumulated number of deaths would also be underestimated (Fig. 3B). Nevertheless, the results from validating the model showed the contrary: the expected death toll is considerably lower than reality (Fig. 5). This is because SCN-1 assumes that new medical tools would be developed and reduce fatality rates by 50%. We acknowledge that this assumption was too optimistic and can be improved in future applications, as more information regarding new medicines/therapeutics is available. Nevertheless, this limitation did not make any difference either in the explosion risk results or in the risk categories, which are based on the number of infections and not on the number of deaths.

We assumed that it is highly unlikely that an infected individual would still be in the transmission period after 2 weeks of infection. New evidence indicates that the transmission period has a considerable chance of being greater than 2 weeks (WHO, 2020c). However, this was a valid assumption when the paper was submitted. For future applications of the model, this can be improved by making changes to the standard deviation of the time to recover parameter, $\sigma(T_{rec})$, which this paper assumed to be zero (Table 2).

There is great uncertainty and lack of clarity regarding how data about the number of confirmed cases in each country have been collected. This can be seen in the high values of standard deviations for the frequency of infection rate per week, especially in the poorest continents (AF and SA). Thus, we acknowledge that the exact order of the hardest-hit continents (Fig. 2) could not be predicted with sufficient accuracy. This may be improved as more tests are performed and more data become available. For the time being, this ranking should be treated only as an initial guide for prioritizing resources among continents. Nevertheless, unlike other models, our approach was able to propagate uncertainty in the global results by using probabilistic language expressed in boxplots (Fig. 2).

DD was modeled in such a way that the frequency of infection, μ^i, per week was assumed to be constant over time until the number of susceptible+infected+recovered individuals reaches a ceiling, and then they remain at that level until a decline in the population (e.g., a random fluctuation or emigration) takes it below the ceiling. This was a simple and conservative way of limiting the growth in the number of infected people. It would be more realistic (although less conservative, in the sense that it will decrease risks) if the frequency of infection, R^i, gradually decreases as the number of recovered individuals increases. This can be improved in future studies by modeling DD as Scramble or Contest-type (Akçakaya et al., 1999), but such DD models have two parameters (not just one as the Ceiling-type), i.e. the maximum growth rate and carrying capacity, and thus more information is necessary in order to be able to estimate such parameters without underestimating risks. Currently, it could be dangerous to model DD as Scramble or Contest as this may lead to underestimated risks.

This paper did not consider the risks of mitigation strategies to the global economy. We quantify and categorize microbial risks only as a measure of the probability of massive infections and

deaths. However, social isolation and business shutdown has caused the income of many people to plunge. There are studies (Mortensen et al., 2016; Rehnberg and Fritzell, 2016; Wolfson et al., 1999) that show a relationship between population income and mortality (e.g., the higher a person's income, the better they can eat and take care of their health and the lower their mortality), and then it is possible to estimate this link and integrate it into our model.

A proposal for future studies would be to include in our model this increased mortality caused by social isolation (and consequent reduction in income) as a way to evaluate questions such as: could economic shutdown kill more people than COVID-19 does? What is the optimum time to maintain business shutdown in order to minimize the total number of deaths caused by both COVID-19 and income reduction?

Currently, our model was built and simulated using a paid software called RAMAS (Akçakaya and Root, 2013). Although we share all the model files (Duarte et al., 2020), it is only useful for those who have the RAMAS license. We acknowledge this impairs the ease of reproducing the model. There is a strong movement towards reproducibility in science, especially regarding near-term ecological forecasting (Anderson et al., 2020; Dietze et al., 2018; White et al., 2019). Therefore, a second proposal for a future line of research is to build and simulate the model in an open scriptable software so that it can be easily reproduced by others.

Other proposals for future studies include: conducting a sensitivity analysis to identify the most important control measures; and undertaking a long-term QMRA of COVID-19 to evaluate the effectiveness of alternative vaccine types and mass vaccination programs.

Conclusions

We have quantified, assessed, categorized and ranked the risks related to varying mitigation scenarios for the future, and provide the results so that authorities can make informed decisions regarding the consequences of these risks. Not only global risks were assessed, but also continent-specific risks, which was useful as an initial guide for prioritizing resources among continents. The model was validated by comparing the results with real values from the six-week period from March 17 - April 28 2020. This showed that the predicted number of infections for a moderate mitigation scenario has been consistent with reality. On the other hand, the predicted number of deaths has been lower than reality, mainly because we were too optimistic by assuming that medical tools would be developed and these would reduce fatality rates.

The main advantage of using this model in comparison to others is that it is probabilistic by nature, so it provides results that incorporate the indelible uncertainty in COVID-19 dynamics. The main limitation is the great uncertainty in the results, which is a consequence of the great uncertainty around data. This is also a limitation of all other models in the literature that use public data on the daily number of confirmed cases per country. Nevertheless, unlike other approaches, our model is able to inform managers about where there is uncertainty in the results, so they can understand the risks arising from their decisions.

Our model did not attempt to make precise predictions, but rather it is only descriptive. Indeed, it is a tool for describing the dynamics of COVID-19 under predefined scenarios (different conditions of social isolation, travel restrictions, medical tools), in order to evaluate the role of such conditions, and to produce meaningful conclusions that can be used to steer public health decisions. Hence, the model is meaningful for decisions taken under uncertainty, but it is very important that due care is taken over how to interpret results.

The main next steps for our model are: to include the effect of varying COVID-19 candidate vaccines and mass vaccination programs and then to conduct a longer term QMRA (e.g., 10 years) in order to evaluate the effectiveness of such vaccines and vaccination programs; and to build and simulate the model in an open scriptable software.

We consider that our model can be used by others and that unusually it could be important to update results every week as more information become available, given the seriousness of the pandemic.

Acknowledgments

The authors are grateful to the National Agency for Research (CNPq-Brazil) for the financial support by means of research grants. This study was financed partially by the Coordenação de Aperfeiçoamento de Pessoal de Nível Superior - Brasil (CAPES) - Finance Code 001.

References

Akçakaya, H.R., Burgman, M.A., Ginzburg, L.R., 1999. Applied Population Ecology, 2nd ed. Sinauer Associates, Sunderland, massachusetts.

Akçakaya, H.R., Root, W.T., 2013. RAMAS GIS: Linking Spatial Data with Population Viability Analysis (version 6). Applied Biomathematics, Setauket, New York.

Altaf, M., Atangana, A., 2020. Modeling the dynamics of novel coronavirus (2019-nCov) with fractional derivative. Alexandria Eng. J. https://doi.org/10.1016/j.aej.2020.02.033

Anderson, B., Chamberlain, S., Krystalli, A., Mullen, L., Ram, K., Ross, N., Salmon, M., Vidoni, M., 2020. rOpenSci Packages: Development, Maintenance, and Peer Review [WWW Document]. 26/04. URL https://devguide.ropensci.org/ (accessed 4.26.20).

Aven, T., Bouder, F., 2020. The COVID-19 pandemic: how can risk science help? J. Risk Res. 1–6. https://doi.org/10.1080/13669877.2020.1756383

Baud, D., Qi, X., Nielsen-Saines, K., Musso, D., Pomar, L., Favre, G., 2020. Real estimates of mortality following COVID-19 infection. Lancet Infect. Dis. https://doi.org/https://doi.org/10.1016/S1473-3099(20)30195-X

Bird, M., Emont, J., Li, S., 2020. China Is Open for Business, but the Postcoronavirus Reboot Looks Slow and Rocky [WWW Document]. march 26. URL https://www.wsj.com/articles/china-is-open-for-business-but-the-post-coronavirus-reboot-looks-slow-and-rocky-11585232600 (accessed 4.27.20).

Boldog, P., Tekeli, T., Vizi, Z., Dénes, A., Bartha, F.A., Röst, G., 2020. Risk Assessment of Novel Coronavirus COVID-19 Outbreaks Outside China. J. Clin. Med. 9, 571. https://doi.org/10.3390/jcm9020571

Burgman, M.A., Ferson, S., Akçakaya, H.R., 1993. Risk assessment in conservation biology. Chapman and Hall, London.

Chen, P., Mao, L., Nassis, G.P., Harmer, P., Ainsworth, B.E., Li, F., 2020. Wuhan coronavirus (2019-nCoV): The need to maintain regular physical activity while taking precautions. J. Sport Heal. Sci. 9, 103–104. https://doi.org/10.1016/j.jshs.2020.02.001

Chen, T.M., Rui, J., Wang, Q.P., Zhao, Z.Y., Cui, J.A., Yin, L., 2020. A mathematical model for simulating the phase-based transmissibility of a novel coronavirus. Infect. Dis. Poverty 9, 1–8. https://doi.org/10.1186/s40249-020-00640-3

Choi, S.C., Ki, M., 2020. Estimating the reproductive number and the outbreak size of Novel Coronavirus disease (COVID-19) using mathematical model in Republic of Korea. Epidemiol Heal. e2020011-0. https://doi.org/10.4178/epih.e2020011

CPR18E, 2005. Guideline for quantitative risk assessment (the “Purple book”), 3rd ed. Publicatiereeks Gevaarlijke Stoffen – PGS.

Dietze, M.C., Fox, A., Beck-Johnson, L.M., Betancourt, J.L., Hooten, M.B., Jarnevich, C.S., Keitt, T.H., Kenney, M.A., Laney, C.M., Larsen, L.G., Loescher, H.W., Lunch, C.K., Pijanowski,

B.C., Randerson, J.T., Read, E.K., Tredennick, A.T., Vargas, R., Weathers, K.C., White, E.P., 2018. Iterative near-term ecological forecasting: Needs, opportunities, and challenges. Proc. Natl. Acad. Sci. 115, 1424 LP – 1432. https://doi.org/10.1073/pnas.1710231115

Duarte, H., Droguett, E., Chagas, M., Siqueira, P.G., Júnior, J.C., 2019. A novel quantitative ecological and microbial risk assessment methodology: theory and practice. Hum. Ecol. Risk Assess. 1–24. https://doi.org/10.1080/10807039.2019.1596736

Duarte, H., Droguett, E.L., Moura, M., de Souza Gomes, E.C., Barbosa, C., Barbosa, V., Araújo, M., 2014. An ecological model for quantitative risk assessment for schistosomiasis: The case of a patchy environment in the coastal tropical area of Northeastern Brazil. Risk Anal. 34, 831–846. https://doi.org/10.1111/risa.12139

[Dataset] Duarte H.O., Siqueira P.G.S.C., Oliveira A.C.A., Moura M.J.C., 2020. Probabilistic Model for Quantitative Risk Assessment of COVID-19 : the case of a patchy environment with potential for migration between continents - Dataset. Mendeley Data, v1. [WWW Document]. 2020. https://doi.org/10.17632/3gyxtcbnj7.1

EPA, 1998. Guidelines for Ecological Risk Assessment. Washington, DC.

Ferguson, N.M., Laydon, D., Nedjati-Gilani, G., Imai, N., Ainslie, K., Baguelin, M., Bhatia, S., Boonyasiri, A., Cucunubá, Z., Cuomo-Dannenburg, G., Dighe, A., Dorigatti, I., Fu, H., Gaythorpe, K., Green, W., Hamlet, A., Hinsley, W., Okell, L.C., Van Elsland, S., Thompson, H., Verity, R., Volz, E., Wang, H., Wang, Y., Gt Walker, P., Walters, C., Winskill, P., Whittaker, C., Donnelly, C.A., Riley, S., Ghani, A.C., 2020. Impact of non-pharmaceutical interventions (NPIs) to reduce COVID-19 mortality and healthcare demand 20. https://doi.org/10.25561/77482

Fujiwara, M., Takada, T., 2017. Environmental Stochasticity. eLS, Major Reference Works. https://doi.org/doi:10.1002/9780470015902.a0021220.pub2

Haas, C.N., Rose, J.B., Gerba, C.P., 1999. Quantitative Microbial Risk Assessment. John Wiley & Sons, New York, USA.

IUCN, 2001. IUCN Red List Categories: Version 3.1. IUCN Species Survival Comission, Gland, Switzerland and Cambridge, UK.

JH, 2020. 2019 NovelCOVID-19 (2019-nCoV) Data Repository [WWW Document]. Johns Hopkins. URL https://github.com/CSSEGISandData/COVID-19 (accessed 3.25.20).

Kalos, M.H., Whitlock, P.A., 2008. Monte Carlo Methods. Wiley-VCH, Weinheim.

Kupferschmidt, K., Cohen, J., 2020. Can China's COVID-19 strategy work elsewhere? Science 367, 1061–1062. https://doi.org/10.1126/science.367.6482.1061

Lan, L., Xu, D., Ye, G., Xia, C., Wang, S., Li, Y., Xu, H., 2020. Positive RT-PCR Test Results in Patients Recovered From COVID-19. JAMA. https://doi.org/10.1001/jama.2020.2783

Lauer, S.A., Grantz, K.H., Bi, Q., Jones, F.K., Zheng, Q., Meredith, H.R., Azman, A.S., Reich, N.G., Lessler, J., 2020. The Incubation Period of Coronavirus Disease 2019 (COVID-19) From Publicly Reported Confirmed Cases: Estimation and Application. Ann. Intern. Med. https://doi.org/10.7326/M20-0504

Lin, Q., Zhao, S., Gao, D., Lou, Y., Yang, S., Musa, S.S., Wang, M.H., Cai, Y., Wang, W., Yang, L., He, D., 2020. A conceptual model for the coronavirus disease 2019 (COVID-19) outbreak in Wuhan, China with individual reaction and governmental action. Int. J. Infect.

Dis. 93, 211–216. https://doi.org/10.1016/j.ijid.2020.02.058

Machado, K., 2020. Covid-19 be damned, Asia's top VC says it's open for business [WWW Document]. 21 April. URL https://www.techinasia.com/covid19-damned-asias-top-vc-theyre-open-business (accessed 4.28.20).

Mortensen, L.H., Rehnberg, J., Dahl, E., Diderichsen, F., Elstad, J.I., Martikainen, P., Rehkopf, D., Tarkiainen, L., Fritzell, J., 2016. Shape of the association between income and mortality: a cohort study of Denmark, Finland, Norway and Sweden in 1995 and 2003. BMJ Open 6, e010974. https://doi.org/10.1136/bmjopen-2015-010974

Pang, J., Wang, M.X., Ang, I.Y.H., Tan, S.H.X., Lewis, R.F., Chen, J.I.-P., Gutierrez, R.A., Gwee, S.X.W., Chua, P.E.Y., Yang, Q., Ng, X.Y., Yap, R.K., Tan, H.Y., Teo, Y.Y., Tan, C.C., Cook, A.R., Yap, J.C.-H., Hsu, L.Y., 2020. Potential Rapid Diagnostics, Vaccine and Therapeutics for 2019 Novel Coronavirus (2019-nCoV): A Systematic Review. J. Clin. Med. 9. https://doi.org/10.3390/jcm9030623

Peng, L., Yang, W., Zhang, D., Zhuge, C., Hong, L., 2020. Epidemic analysis of COVID-19 in China by dynamical modeling 1–18.

Population Pyramid, 2019. Population Pyramids of the World 2019 [WWW Document]. URL https://www.populationpyramid.net/ (accessed 3.25.20).

Rehnberg, J., Fritzell, J., 2016. The shape of the association between income and mortality in old age: A longitudinal Swedish national register study. SSM - Popul. Heal. 2, 750–756. https://doi.org/10.1016/j.ssmph.2016.10.005

Sohrabi, C., Alsafi, Z., O'Neill, N., Khan, M., Kerwan, A., Al-Jabir, A., Iosifidis, C., Agha, R., 2020. World Health Organization declares global emergency: A review of the 2019 novel coronavirus (COVID-19). Int. J. Surg. 76, 71–76. https://doi.org/10.1016/j.ijsu.2020.02.034

Spreeuwenberg, P., Kroneman, M., Paget, J., 2018. Reassessing the Global Mortality Burden of the 1918 Influenza Pandemic. Am. J. Epidemiol. 187, 2561–2567. https://doi.org/10.1093/aje/kwy191

Taleb, N.N., 2007. The black swan: The impact of the highly improbable, The Black Swan: The Impact of the Highly Improbable. Random House & Penguin, Paris. https://doi.org/10.4324/9781912281206

Teaf, C., Kuperberg, M., 2004. Risk Assessment, Risk Management & Risk Communication. https://doi.org/10.1007/978-94-007-1050-4_1

The Inquirer, 2020. Asia shares mixed, eyeing economies reopening, central banks [WWW Document]. April 28. URL https://business.inquirer.net/295920/asia-shares-mixed-eyeing-economies-reopening-central-banks (accessed 4.28.20).

Time24, 2020. Bolsonaro says he will end confinement by coronavirus: "Orientation will be vertical isolation" [WWW Document]. URL https://www.time24.news/n24/2020/03/bolsonaro-says-he-will-end-confinement-by-coronavirus-orientation-will-be-vertical-isolation.html (accessed 3.25.20).

Toms, C., Petrie, S., 2020. COVID-19 , Australia : Epidemiology Report 6 [WWW Document].

UNWTO, 2019. International Tourist Arrivals by (Sub)region. World Tour. Barom. 17, 44. https://doi.org/https://www.e-unwto.org/doi/pdf/10.18111/wtobarometereng.2019.17.1.4

Vital Surveillances, 2020. The epidemiological characteristics of an outbreak of 2019 novel coronavirus diseases (COVID-19) in China. China CDC Wkly. 2, 113–122. https://doi.org/https://cdn.onb.it/2020/03/COVID-19.pdf.pdf

Walker, P., Whittaker, C., Watson, O., Baguelin, M., Ainslie, K., Bhatia, S., Boonyasiri, A., Boyd, O., Cattarino, L., Cucunubá, Z., Cuomo-dannenburg, G., 2020. The Global Impact of COVID-19 and Strategies for Mitigation and Suppression 1–19. https://doi.org/https://doi.org/10.25561/77482

Wells, C.R., Sah, P., Moghadas, S.M., Pandey, A., Shoukat, A., Wang, Y., Wang, Z., Meyers, L.A., Singer, B.H., Galvani, A.P., 2020. Impact of international travel and border control measures on the global spread of the novel 2019 coronavirus outbreak. Proc. Natl. Acad. Sci. 117, 7504 LP – 7509. https://doi.org/10.1073/pnas.2002616117

White, E.P., Yenni, G.M., Taylor, S.D., Christensen, E.M., Bledsoe, E.K., Simonis, J.L., Ernest, S.K.M., 2019. Developing an automated iterative near-term forecasting system for an ecological study. Methods Ecol. Evol. 10, 332–344. https://doi.org/10.1111/2041-210X.13104

WhiteHouse, 2020. Press Briefing by Members of the President's Coronavirus Task Force [WWW Document]. January 31, 2020. URL https://www.whitehouse.gov/briefings-statements/press-briefing-members-presidents-coronavirus-task-force/

WHO, 2020a. Coronavirus disease 2019 situation report - 51, World Health Organization. https://doi.org/10.1001/jama.2020.2633

WHO, 2020b. Coronavirus disease 2019 situation report - 63, World Health Organization. https://doi.org/10.1001/jama.2020.2633

WHO, 2020c. Coronavirus disease 2019 - Report 73, World Health Organization. https://doi.org/10.1001/jama.2020.2633

WHO, 2019. Past pandemics [WWW Document]. World Heal. Organ. URL http://www.euro.who.int/en/health-topics/communicable-diseases/influenza/pandemic-influenza/past-pandemics (accessed 3.25.20).

WHO, 2016. Quantitative Microbial Risk Assessment: Application for Water Safety Management. World Heal. Organ. 202. https://doi.org/10.1002/9781118910030

WHO, 2005. Ten things you need to know about pandemic influenza (update of 14 October 2005)., Releve epidemiologique hebdomadaire. Switzerland.

Wolfson, M., Kaplan, G., Lynch, J., Ross, N., Backlund, E., 1999. Relation between income inequality and mortality: empirical demonstration. BMJ 319, 953–955. https://doi.org/10.1136/bmj.319.7215.953

Fig. 1.

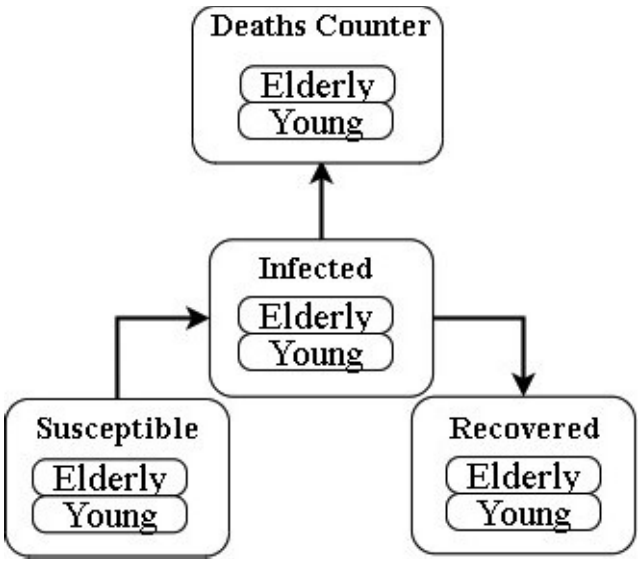

Fig. 1. Simplified schematic representation of Covid-19 dynamics in human population.

Fig. 2

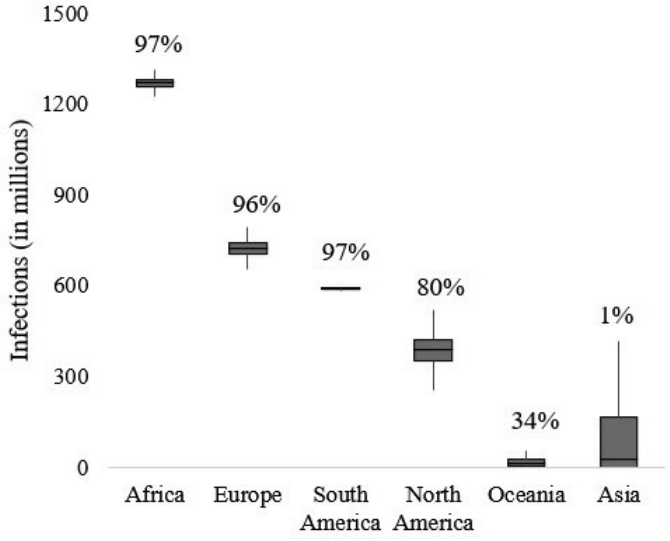

Fig. 2. Boxplots for the number of infections in each continent (in millions) at final time-step (after 52 weeks) for a business as usual scenario (SCN-0). The percentages are the percentage of infections from the total subpopulation in each continent

Fig. 3.

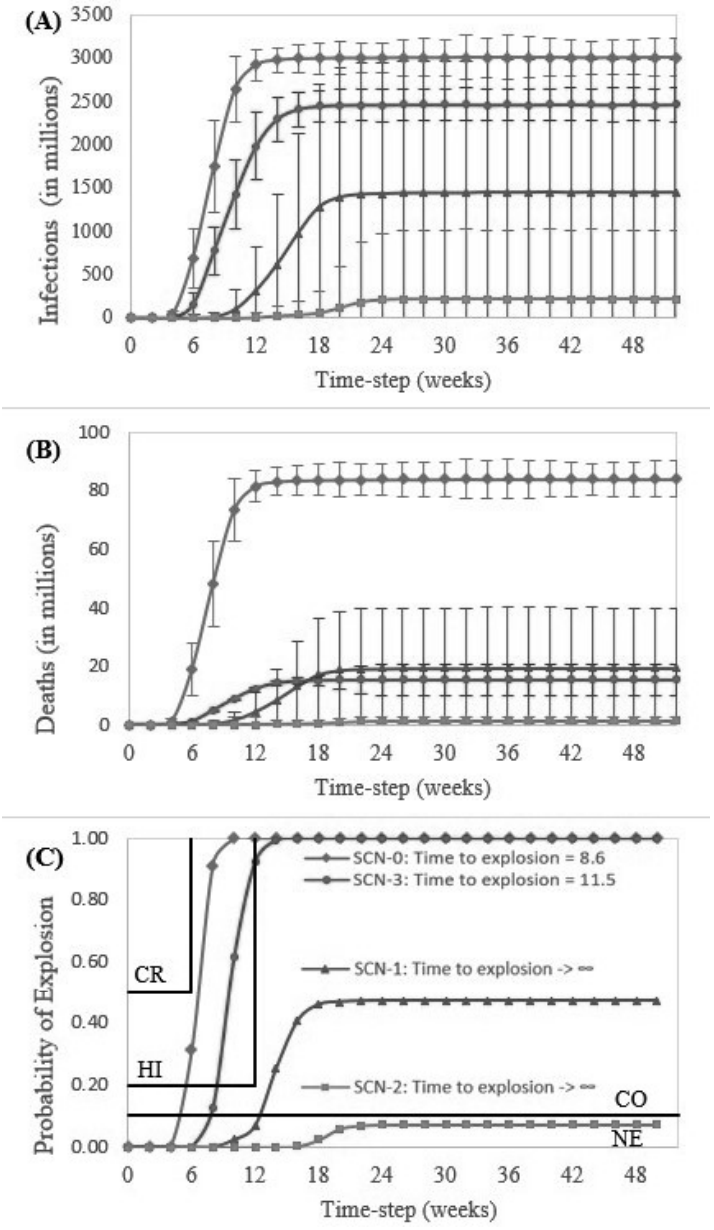

Fig. 3. (A) Number of infected individuals in the world over time; (B) Death toll in the world over time; (C) Time to explosion (CR = Critical Risk; HI = High Risk; CO = Considerable Risk; NE = Negligible Risk). SCN-0 (business as usual); SCN-1 (moderate mitigation); SCN-2 (strong mitigation; SCN-3 (vertical isolation).

Fig. 4.

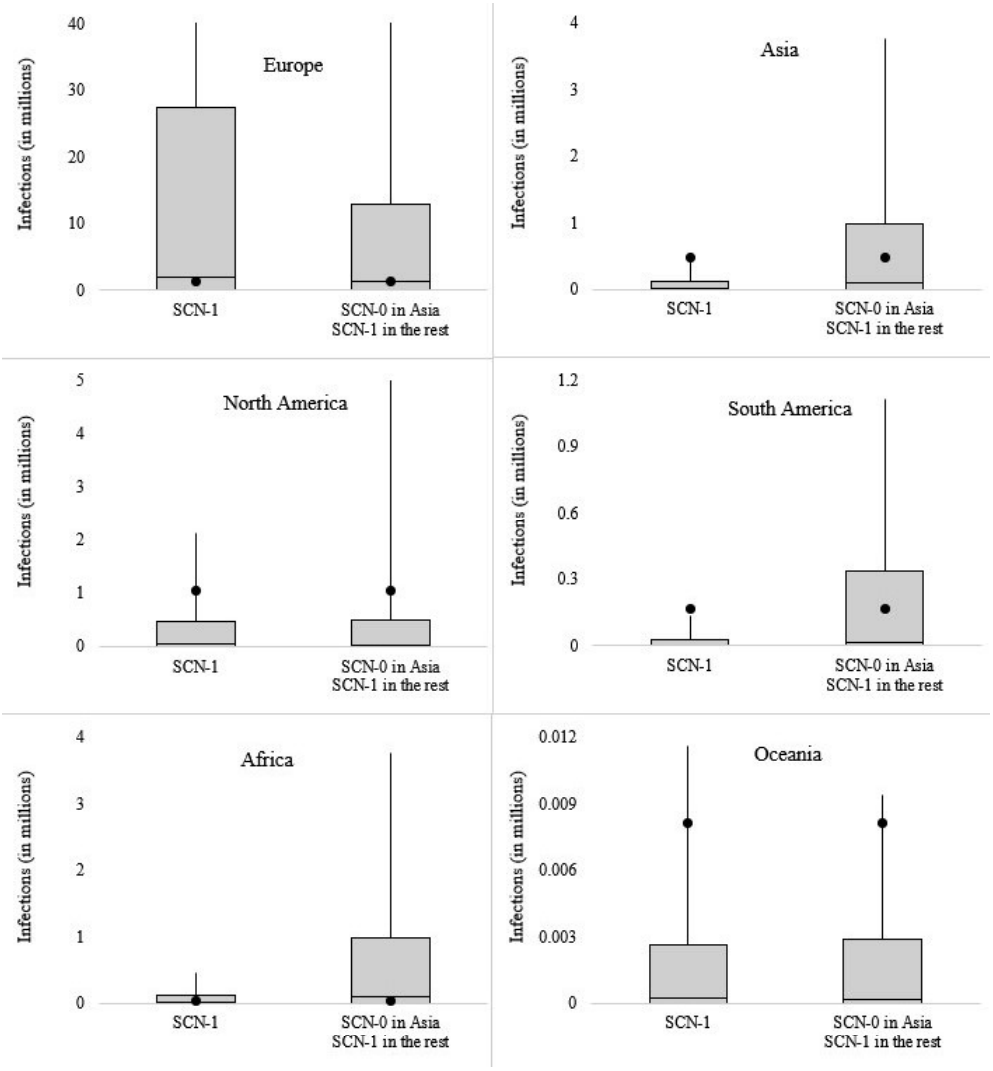

Fig. 4. Validation of the model at week 6 (Apr 28th 2020) for each continent, assuming: SCN-1 in all continents (left boxplot); and SCN-0 only in Asia and SCN-1 in all the other continents (right boxplot). The real values of infections are represented as dots and predicted values as boxplots.

Fig. 5.

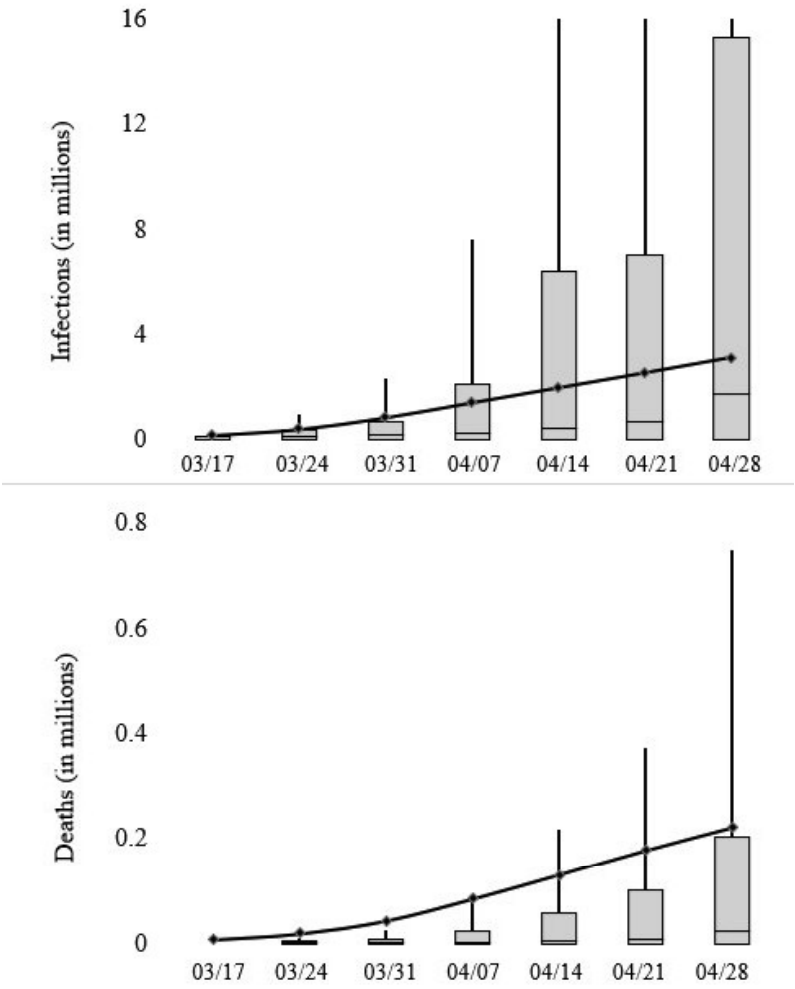

Fig. 5. Validation of the model for the last six weeks at global-level by comparison of the real (solid line) against predicted values (boxplots), for a business as usual SCN-0 in Asia and moderate mitigation SCN-1 in all the other continents: (A) number of infections (in millions); (B) number of deaths (in millions).

Table 1. Definition of variables of the model.

Variable	Symbol	Description
Number of susceptible young in continent i at time t	$N_2^i(t)$	Assessment endpoint described as minimum, average and maximum values, with a 95% confidence interval
Number of infected elderlies in continent i at time t	$N_5^i(t)$	Assessment endpoint described as minimum, average and maximum values, with a 95% confidence interval
Continent-specific frequency of infection	μ^i	Number of expected new cases of infection generated by one infected person in each continent per week
Continent-specific standard deviation from frequency of infection	σ_R^i	Standard deviation of reproductive number
Exposure level for young $(s = 2)$ and elderly $(s = 5)$ for each SCN.	E_s^k	Accounts for the reduction in the exposure due to an SCN k (Table 4)
Ceiling for each continent i	K^i	Total initial population for continent i
Travel restriction for each SCN	T_r	Proportion of flights reduced as a measure to lower the spread of the infection (Figure 3)
Fatality rate for [s=2] and [s=5]	d_i	Proportion of individuals that die from the infection each week
Reduction in fatality-rate due to medical tools	f^k	Reduction in the fatality rate for each SCN k

Note: [s=1] young susceptible, [s=2] young infected, [s=3] young recovered, [s=4] elderly susceptible, [s=5], elderly infected and, [s=6] elderly recovered.

Table 2. Definition of the parameters of the model.

Parameter	Symbol	Assumptions (Data Source or Rationale)	Mean	σ
Age-specific exposure	β_{su}	The probability of the virus being transmitted among young is higher than among elderly (Exposure Assessment section and Table 3).	$\{\beta_{22} = 1\ \beta_{25} = \beta_{52} =$	
Time to recover	T_{rec}	Most individuals take two weeks to recover (37).	2	
Permanence rate from [s=1] to [s=1]; from [s=4] to [s=4]	$a_{11}\,;\, a_{44}$	The susceptible population is much larger than the infected population, so there is a slight decrease in the susceptible population as more people get infected (Educated guess).	0.999	0.001
Infection rate from [s=2] to [s=2]; from [s=5] to [s=5]	$a_{22}^{i}(t);\, a_{55}^{i}(t)$	Directly proportional to the frequency of infection and corrected by the age-specific exposure and recovery rate. Also corrected by the exposure level in each SCN.	$E_2^k(\beta_{22}\mu^i - a_{32});$ $E_5^k(\beta_{55}\mu^i - a_{65})$	$E_5^k(\beta_{22}\sigma_R^i - \sigma_{32})\,;$ $E_5^k(\beta_{55}\sigma_R^i - \sigma_{65})$
Infection rate from [s=5] to [s=2]; from [s=2] to [s=5]	$a_{25}^{i}(t);\, a_{52}^{i}(t)$	Same as $a_{22}^{i}(t);\, a_{55}^{i}(t)$.	$E_2^k(\beta_{25}\mu^i - a_{32});$ $E_5^k(\beta_{52}\mu^i - a_{65})$	$E_2^k(\beta_{25}\sigma_R^i - \sigma_{32});$ $E_5^k(\beta_{52}\sigma_R^i - \sigma_{65})$
Recovery rate from [s=2] to [s=3]; from [s=5] to [s=6]	a_{32};a_{65}	Assessment of frequency section.	$\frac{1}{T_{rec}}(1-\alpha_2);$ $\frac{1}{T_{rec}}(1-\alpha_5)$	
Permanence rate from [s=3] to [s=3]; [s=6] to [s=6]	a_{33};a_{66}	The probability of a recovered individual being re-infected is zero (LAN et al., 2020).	1.0	
Fatality rate of [s=2]; [s=5]	$\alpha_2\,;\,\alpha_5$	Description of SCNs section	$f^k * d_2\,;$ $f^k * d_5$	
Dispersal rate of individuals among continents	m_{ij}	Parameterization of the model and Initial Conditions section	$\left(\frac{M_{ij}}{N^i}\right) \times T_r$	
Threshold for infected population explosion	I_{exp}	Threshold for an undesired consequence (25% of the world population infected)	1,947,531,610	

Note: [s=1] young susceptible, [s=2] young infected, [s=3] young recovered, [s=4] elderly susceptible, [s=5], elderly infected and, [s=6] elderly recovered.

Table 3. Summary of the exposure assessment for each SCN

	Estimated time out of home for any activity (hours/week)		Exposure level		Duration of social isolation (weeks)	
Scenarios	Young	Elderly	Young	Elderly	Young	Elderly
SCN-0	46	23	100%	50%	0	0
SCN-1	8	2	18%	9%	2	7
SCN-2	8	2	18%	9%	7	17
SCN-3	46	0	100%	0%	0	52

Table 4. Frequency of infection per week (mean and standard deviation) for each continent.

	Frequency of infection	
Subpopulation	Mean	SD
Europe	4.3781	2.7887
North America	3.5772	2.6315
South America	10.2265	4.9092
Asia	1.2812	0.3117
Africa	5.3783	3.1823
Oceania	2.2280	1.1916

Table 5. Summary of the outputs for each SCN.

Scenario	Output				
	World Infected Population	Total Death Toll	Risk of Explosion	Time to Explosion	Risk Category
SCN-0 (benchmark)	Fluctuates between approximately 3 and 3.6 billion	Fluctuates between approximately 84 and 88 million	100%	8.6 weeks	HI
SCN-1 (moderate mitigation)	Fluctuates between approximately 1.45 billion and 3.46 billion	Fluctuates between approximately 19.5 and 46.5 million	47.30%	Tends to infinity	CO
SCN-2 (strong mitigation)	Fluctuates between approximately 223 and 910 million	Fluctuates between approximately 1.5 and 6.3 million	7.28%	Tends to infinity	NE
SCN-3 (vertical isolation plan)	Fluctuates between approximately 2.47 and 4.26 billion	Fluctuates between approximately 15.4 and 26.6 million	100%	11.5 weeks	HI
SCN-0 in AS; SCN-1 in the other continents	Fluctuates between approximately 1.67 and 2.71 billion	Fluctuates between approximately 22.5 and 29 million	54.52%	19.8 weeks	CO
SCN-2 in AF; SCN-1 in the other continents	Fluctuates between approximately 1.34 and 2.23 billion	Fluctuates between approximately 37.2 and 62.1 million	50.60%	23.4 weeks	CO
SCN-2 in AF and EU; SCN-1 in the other continents	Fluctuates between approximately 735 million and 2.03 billion	Fluctuates between approximately 20.5 and 56.6 million	27.88%	Tends to infinity	CO

Note: HI = High Risk; CO = Considerable Risk; NE = Negligible Risk

SupplementaryMaterial for

Probabilistic Model for Quantitative Risk Assessment of COVID-19 in the world: the case of a patchy environment with potential for migration among continents

Heitor O. Duarte[a*]; Paulo G. S. C. Siqueira[b,c*]; Alexandre C. A. Oliveira[a]; Márcio J. C. Moura[b,c]

*Corresponding authors

Email: heitorod@gmail.com; psems@hotmail.com; calumbi-oliveira@hotmail.com; marcio@ceerma.org

[a]Department of Mechanical Engineering, Universidade Federal de Pernambuco, Av. Prof. Moraes Rego, 1235 - Cidade Universitária, Recife - PE, 50670-901

[b]CEERMA - Center for Risk Analysis, Reliability and Environmental Modeling, Universidade Federal de Pernambuco, Recife-PE, Brazil

[c]Department of Production Engineering, Universidade Federal de Pernambuco, Rua Acadêmico Hélio Ramos, s/n, Cidade Universitária, CEP: 50740-530 Recife-PE, Brazil

Table A1. Record of infected per day in each continent of interest. Adapted from: (JH, 2020).

Date	Europe	North America	South America	Africa	Asia	Oceania
1/22/20	0	1	0	0	554	0
1/23/20	0	1	0	0	652	0
1/24/20	2	2	0	0	937	0
1/25/20	3	2	0	0	1429	0
1/26/20	3	6	0	0	2105	4
1/27/20	4	6	0	0	2912	5
1/28/20	8	7	0	0	5558	5
1/29/20	10	7	0	0	6143	6
1/30/20	10	7	0	0	8208	9
1/31/20	16	11	0	0	9891	9
2/1/20	20	12	0	0	11993	12
2/2/20	22	12	0	0	16740	12
2/3/20	24	15	0	0	19829	12
2/4/20	25	15	0	0	23838	13
2/5/20	25	16	0	0	27580	13
2/6/20	25	16	0	0	30761	14
2/7/20	28	18	0	0	34268	15
2/8/20	33	18	0	0	36992	15
2/9/20	34	18	0	0	40017	15
2/10/20	39	18	0	0	42553	15
2/11/20	41	19	0	0	44590	15
2/12/20	42	19	0	0	44968	15
2/13/20	42	20	0	0	60114	15
2/14/20	42	20	0	1	66587	15
2/15/20	43	20	0	1	68664	15
2/16/20	43	20	0	1	70788	15
2/17/20	43	21	0	1	72722	15
2/18/20	43	21	0	1	74512	15
2/19/20	43	21	0	1	74936	15
2/20/20	43	21	0	1	75481	15
2/21/20	60	24	0	1	76083	19
2/22/20	102	24	0	1	77794	22
2/23/20	195	24	0	1	78030	22
2/24/20	273	61	0	1	78518	22
2/25/20	373	62	0	2	79257	22
2/26/20	527	68	1	2	80057	22
2/27/20	789	71	1	2	81148	23
2/28/20	1061	75	1	4	82219	24
2/29/20	1420	92	2	4	83718	26
3/1/20	2120	103	9	5	85316	28

3/2/20	2610	130	9	9	86693	31
3/3/20	3194	153	12	12	88559	40
3/4/20	4119	187	17	21	89794	55
3/5/20	5483	259	23	24	91071	58
3/6/20	7108	317	36	43	93120	64
3/7/20	9150	462	44	43	94858	68
3/8/20	11526	589	73	86	96071	81
3/9/20	13912	667	84	94	96939	96
3/10/20	16693	1045	105	106	98138	112
3/11/20	21184	1397	147	122	99903	133
3/12/20	21912	1792	182	138	101207	133
3/13/20	33073	2384	354	176	103065	205
3/14/20	40113	2951	439	254	104982	256
3/15/20	47100	3792	502	320	106913	305
3/16/20	55715	5100	731	410	108513	386
3/17/20	76870	7166	1045	528	110493	464
3/18/20	90528	8751	1162	652	112517	588
3/19/20	108928	14891	1652	841	114974	710
3/20/20	129446	20621	2268	1042	117245	832
3/21/20	150950	27530	3013	1250	119944	1125
3/22/20	169466	35733	4146	1511	123004	1383
3/23/20	169334	35798	4164	1568	123045	1383

Table A2. Dispersal matrix between continents. Each element in the dispersal matrix means that x.xx% of the population of continent j (column) travels to continent i (line) per week.

	AS	EU	SA	NA	OC	AF
AS		0.00026	0.000365	0.000399	0.000208	0.000256
EU	0.000355		0.000456	0.000996	0.000260	0.000256
SA	0.000025	0.00026		0.000399	0.000104	0.000034
NA	0.000209	0.00091	0.000456		0.000260	0.000342
OC	0.000008	0.00010	0.000046	0.000199		0.000017
AF	0.000021	0.00016	0.000091	0.000266	0.000156	

Figure A1

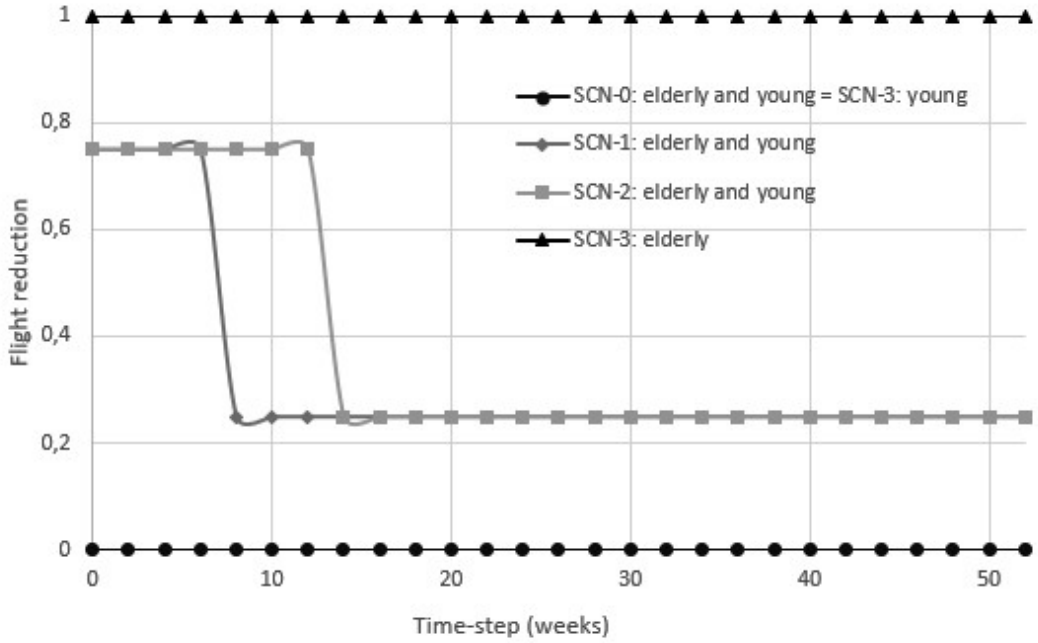

Figure S1. Flight restriction over time, $T_r(t)$, for each scenario: SCN-0 (business as usual), SCN-1 (moderate mitigation), SCN-2 (strong mitigation) and SCN-3 (vertical isolation).